

2D-Magnetic Field and Biaxial In-Plane Pre-Load Effects on the Vibration of Double Bonded Orthotropic Graphene Sheets

A.H. Ghorbanpour Arani¹, M.J. Maboudi¹, A. Ghorbanpour Arani^{1,2*}, S. Amir¹

¹Faculty of Mechanical Engineering, University of Kashan, Kashan, Islamic Republic of Iran

²Institute of Nanoscience & Nanotechnology, University of Kashan, Kashan, Islamic Republic of Iran

Received 5 April 2013; accepted 29 May 2013

ABSTRACT

In this study, thermo-nonlocal vibration of double bonded graphene sheet (DBGS) subjected to 2D-magnetic field under biaxial in-plane pre-load are presented. The elastic forces between layers of graphene sheet (GS) are taken into account by Pasternak foundation and the classical plate theory (CLPT) and continuum orthotropic elastic plate are used. The nonlocal theory of Eringen and Maxwell's relations are employed to incorporate the small-scale effect and magnetic field effects, respectively, into the governing equations of the GSs. The differential quadrature method (DQM) is used to solve the governing differential equations for simply supported edges. The detailed parametric study is conducted, focusing on the remarkable effects of the angle and magnitude of magnetic field, different type of loading condition for couple system, tensile and compressive in-plane pre-load, aspect ratio and nonlocal parameter on the vibration behavior of the GSs. The result of this study can be useful to design of micro electro mechanical systems and nano electro mechanical systems.

© 2013 IAU, Arak Branch. All rights reserved.

Keywords: Nonlocal vibration; Thermo-nonlocal; Couple system; 2D-magnetic field; Biaxial in-plane pre-load

1 INTRODUCTION

CARBON nanostructures such as GSs and carbon nanotubes (CNTs) have many special and superior physical, chemical and mechanical properties, for example high electrical and thermal conduction, exceptional stiffness and strength, and low density. Besides, they have a huge potential in electrical and mechanical applications such as sensors, semiconductor devices, aeronautic and astronautic technology, automobile, and many other modern industries. Nanotubes are deformed GS and it is another reason that makes more interest to analyze these structures. Vibration analysis of orthotropic GS embedded in Pasternak elastic medium using nonlocal elasticity theory and DQM has been studied by Pradhan and Kumar [1] who investigated the effects of nonlocal parameter, size of the graphene sheets, stiffness of surrounding medium and boundary conditions on non-dimensional vibration frequencies. Murmu and Adhikari [2] investigated axial instability of double-nanobeam-systems. Analysis of the scale effects in buckling loads of double-nanobeam-system with synchronous and asynchronous modes has been discussed in their study. Also they studied [3] the nonlocal vibration of bonded double-nanoplate-systems that two nanoplates are assumed to be bonded by an enclosing elastic medium. Their work provided a starting point for further investigation of more complex nanoplates systems with graphene based. The effect of in-plane pre-load on vibration of plate, nanotubes and beams was investigated by some researchers [4-6]. Free vibration of functionally graded beams with piezoelectric layers subjected to axial load studied by Karami Khorramabadi [7] who presented

* Corresponding author. Tel.: +98 913 162 6594; Fax: +98 361 591 2424.
E-mail address: aghorban@kashanu.ac.ir (A.Ghorbanpour Arani).

the effects of the constituent volume fractions, influences of applied voltage and axial compressive loads on the vibration frequency. Murmu and Pradhan [8] investigated vibration analysis of nanoplates under uniaxial prestressed conditions. Influences of small scale and uniaxial pre-load on the nonlocal frequency solutions studied. Also, Kiani [9] studied vibration of double-walled carbon nanotubes on elastic foundation subjected to axial load.

Recently, influence of magnetic field on GS and CNTs behavior is attracted many researchers [10-15] so that some experiments performed on CNTs under an electro-magnetic field [16-19]. Kiani [20] studied transverse wave propagation in elastically confined single-walled carbon nanotubes subjected to longitudinal magnetic fields using nonlocal elasticity models. Their results showed the influence of longitudinal magnetic field on the characteristics of both flexural and shear waves in SWCNTs embedded in an elastic matrix. Murmu et al. [21] expressed the influence of an in-plane magnetic field on the transverse vibration of a magnetically sensitive single-layer graphene sheet (SLGS) embedded in a Winkler medium using equivalent continuum nonlocal elastic plate theory and considering the Lorentz magnetic force obtained from Maxwell's relation. They reported effects of the in-plane magnetic field on higher natural frequencies and different aspect ratios of SLGS.

Motivated by these considerations, in the present study, in order to improve optimum design of nanostructures, the effect of 2D-magnetic field and different loading condition by biaxial in-plane pre-load on vibration of orthotropic DBGS resting on Pasternak foundation is examined. Using nonlocal elasticity orthotropic classical plate theory and Maxwell's Relations, the motion equations are derived based on energy method and Hamilton's principle using DQ approach. The effects of loading condition, finally, the magnetic angle, the magnetic parameter and nonlocal parameter are investigated.

2 FUNDAMENTAL EQUATIONS

2.1 The classical plate theory

In this study, a DBGS with 2D-magnetic field under in-plane pre-load and resting on a Pasternak foundation is shown in Fig. 1(a), which geometrical parameters are also indicated in Fig. 1(b). The Pasternak foundation has been simulated by containing spring constants of Winkler-type (k_w), shear constants of Pasternak-type (k_g).

According to the classical plate theory (CLPT), displacement field may be written as [22]:

$$u_x(x, y, z, t) = -z \frac{\partial w(x, y, t)}{\partial x}, \quad u_y(x, y, z, t) = -z \frac{\partial w(x, y, t)}{\partial y}, \quad u_z(x, y, z, t) = w(x, y, t) \quad (1)$$

where u_x , u_y and u_z are displacements in x , y and z directions, respectively. Using Eq. (1), the strain-displacement relations according to von Kármán strains, can be expressed as:

$$\begin{aligned} \varepsilon_{xx} &= \frac{\partial u_x}{\partial x} = -z \frac{\partial^2 w}{\partial x^2}, & \varepsilon_{yy} &= \frac{\partial u_y}{\partial y} = -z \frac{\partial^2 w}{\partial y^2}, & \varepsilon_{zz} &= \frac{\partial u_z}{\partial z} = 0 \\ \gamma_{xy} &= \frac{\partial u_x}{\partial y} + \frac{\partial u_y}{\partial x} = -2z \frac{\partial^2 w}{\partial y \partial x}, & \gamma_{yz} &= \frac{\partial u_y}{\partial z} + \frac{\partial u_z}{\partial y} = 0, & \gamma_{xz} &= \frac{\partial u_x}{\partial z} + \frac{\partial u_z}{\partial x} = 0 \end{aligned} \quad (2)$$

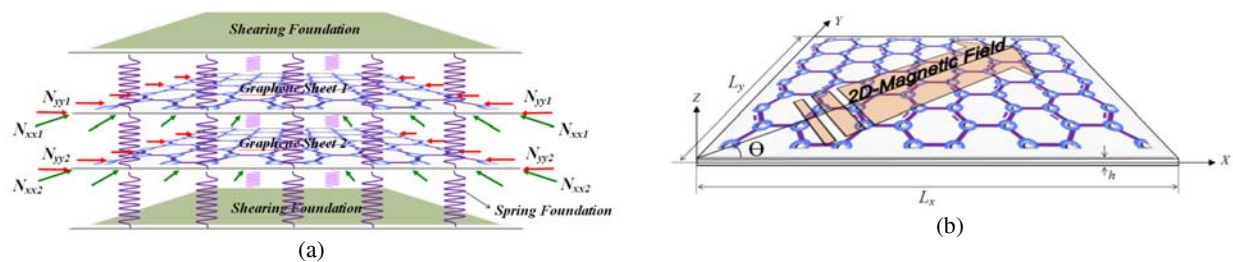


Fig. 1

(a) Schematic of DBGS in Pasternak foundation under biaxial in-plane pre-load and 2D magnetic field (b) Geometric parameters of SLGS subjected to 2D magnetic field.

2.2 Nonlocal elasticity plate theory

In the Eringen’s nonlocal elasticity model, the stress state at a reference point in the body is regarded to be dependent not only on the strain state at this point, but also on the strain states at all of the points throughout the body. The basic equations for homogeneous, isotropic and nonlocal elastic solid with zero body forces are given by [23]

$$\sigma_{ij,j} = 0 \quad \sigma_{ij}(x) = \int \alpha(|x - x'|, \tau) C_{ijkl} \varepsilon_{kl}(x') dV(x'), \quad \forall x \in V \quad \varepsilon_{ij} = \frac{1}{2}(u_{i,j} + u_{j,i} + u_{k,i}u_{k,j}) \quad (3)$$

where C_{ijkl} is the elastic module tensor of classical (local) isotropic elasticity; σ_{ij} and ε_{ij} are stress and strain tensors, respectively, and u_i is displacement vector. $\alpha(|x - x'|, \tau)$ is the nonlocal modulus. $|x - x'|$ is the Euclidean distance, and $\tau = e_0 a / l$ is defined that l is the external characteristic length, e_0 denotes a constant appropriate to each material, and a is an internal characteristic length of the material (e. g. , length of C-C bond, lattice spacing, granular distance). Consequently, $e_0 a$ is a constant parameter which is obtained with molecular dynamics, experimental results, experimental studies and molecular structure mechanics. The constitutive equation of the nonlocal elasticity can be written as [23].

$$\begin{pmatrix} \sigma_{xx}^{nl} \\ \sigma_{yy}^{nl} \\ \sigma_{xy}^{nl} \end{pmatrix} - (e_0 a)^2 \nabla^2 \begin{pmatrix} \sigma_{xx}^{nl} \\ \sigma_{yy}^{nl} \\ \sigma_{xy}^{nl} \end{pmatrix} = \begin{pmatrix} \frac{E_{11}}{1 - \nu_{12}\nu_{21}} & \frac{E_{22}\nu_{12}}{1 - \nu_{12}\nu_{21}} & 0 \\ \frac{E_{22}\nu_{12}}{1 - \nu_{12}\nu_{21}} & \frac{E_{22}}{1 - \nu_{12}\nu_{21}} & 0 \\ 0 & 0 & G_{12} \end{pmatrix} \begin{pmatrix} \varepsilon_{xx} - \alpha_x \Delta T \\ \varepsilon_{yy} - \alpha_y \Delta T \\ \gamma_{xy} \end{pmatrix} \quad (4)$$

where α_i ($i = x, y$) denotes linear thermal expansion of coefficient in x and y directions, respectively, and σ^{nl} is nonlocal stresses. It should be noted that the nonlocal stress tensor becomes a local one when the nonlocal parameter is zero ($e_0 a = 0$). Using the Eringen's nonlocal theory, the nonlocal stress resultant can be rewritten as [23]:

$$\begin{aligned} (1 - (e_0 a)^2 \nabla^2)(M_{ii}, N_{ii}) &= \int_{\frac{-h}{2}}^{\frac{+h}{2}} \sigma_{ii}(z, 1) dz & i = x, y \\ (1 - (e_0 a)^2 \nabla^2)(M_{xy}, N_{xy}) &= \int_{\frac{-h}{2}}^{\frac{+h}{2}} \sigma_{xy}(z, 1) dz \end{aligned} \quad (5)$$

$N_{ii} = N_{ii}^m + N_{ii}^T$ ($i = x, y$) is resultant force where N_{ii}^m and N_{ii}^T are mechanical and thermal resultant forces in which defines as [8]:

$$N_{xx}^m = -P \quad , \quad N_{yy}^m = -kP \quad , \quad N_{xx}^T = -c_{11}\alpha_x \Delta T - c_{12}\alpha_y \Delta T \quad , \quad N_{yy}^T = -c_{12}\alpha_x \Delta T - c_{22}\alpha_y \Delta T \quad (6)$$

2.3 Maxwell's relations

The governing electro-dynamic Maxwell equations for a perfectly conducting elastic body can be written as [15, 24]:

$$\vec{J} = \nabla \times \vec{h}, \quad \nabla \times \vec{e} = -\eta \frac{\partial \vec{h}}{\partial t}, \quad \nabla \cdot \vec{h} = 0 \quad (7)$$

where \vec{J} , \vec{U} and η indicate the current density, the vector of displacement ($\vec{U} = (u_x, u_y, u_z)$) and magnetic field permeability, respectively. Also \vec{e} is strength vectors of electric field and \vec{h} is disturbing vectors of magnetic field, that defined as [15, 24]:

$$\vec{e} = -\eta \left(\frac{\partial \vec{U}}{\partial t} \times \vec{H} \right) \quad \vec{h} = \nabla \times (\vec{U} \times \vec{H}) \quad (8)$$

Due to applying 2D magnetic field in any direction in this study, we consider $\vec{H} = (H_x, H_y, 0)$ that act on DBGS, which:

$$\left. \begin{aligned} H_x &= H \cos \theta \\ H_y &= H \sin \theta \end{aligned} \right\} \Rightarrow H^2 = H_x^2 + H_y^2 \quad (9)$$

where H is the magnitude of total applied magnetic field and θ is angle of between direction of 2D magnetic field and positive x -axis Fig.1(b). Considering Eq.(9) and using Hamilton arithmetic operator ($\nabla = \frac{\partial}{\partial x} \hat{i} + \frac{\partial}{\partial y} \hat{j} + \frac{\partial}{\partial z} \hat{k}$), Eq. (8) yields:

$$\vec{h} = \left(H_y \frac{\partial u_x}{\partial y} - H_x \frac{\partial u_y}{\partial y} - H_x \frac{\partial u_z}{\partial z} \right) \hat{i} + \left(-H_y \frac{\partial u_z}{\partial z} - H_y \frac{\partial u_x}{\partial x} + H_x \frac{\partial u_y}{\partial x} \right) \hat{j} + \left(H_x \frac{\partial u_z}{\partial x} + H_y \frac{\partial u_z}{\partial y} \right) \hat{k} \quad (10)$$

$$\begin{aligned} \vec{J} &= \left(H_x \frac{\partial^2 u_z}{\partial x \partial y} + H_y \frac{\partial^2 u_z}{\partial y^2} + H_y \frac{\partial^2 u_z}{\partial z^2} + H_y \frac{\partial^2 u_x}{\partial x \partial z} - H_x \frac{\partial^2 u_y}{\partial x \partial z} \right) \hat{i} \\ &+ \left(H_y \frac{\partial^2 u_x}{\partial y \partial z} - H_x \frac{\partial^2 u_y}{\partial y \partial z} - H_x \frac{\partial^2 u_z}{\partial z^2} - H_x \frac{\partial^2 u_z}{\partial x^2} - H_y \frac{\partial^2 u_z}{\partial x \partial y} \right) \hat{j} \\ &+ \left(-H_y \frac{\partial^2 u_z}{\partial z \partial x} - H_y \frac{\partial^2 u_x}{\partial x^2} + H_x \frac{\partial^2 u_y}{\partial x^2} - H_y \frac{\partial^2 u_x}{\partial y^2} + H_x \frac{\partial^2 u_y}{\partial y^2} + H_x \frac{\partial^2 u_z}{\partial y \partial z} \right) \hat{k} \end{aligned} \quad (11)$$

By setting α, β and γ into Eq. (11) so that $\vec{J} = \alpha \hat{i} + \beta \hat{j} + \gamma \hat{k}$, the Lorentz force (\vec{f}) caused by the 2D-magnetic field is given as:

$$\vec{f} = (f_x, f_y, f_z) = \eta (\vec{J} \times \vec{H}) \quad \vec{f} = \eta \left(-\gamma H_y \hat{i} + \gamma H_x \hat{j} + (\alpha H_y - \beta H_x) \hat{k} \right) \quad (12)$$

For transverse vibration considered Lorentz force in z direction and using Eq. (1), the lateral force produced by magnetic field can be written as [21]:

$$q_{magnetic} = \int_{-\frac{h}{2}}^{+\frac{h}{2}} f_z dz = \eta h \left(4 H_x H_y \frac{\partial^2 w}{\partial x \partial y} + H_y^2 \frac{\partial^2 w}{\partial y^2} - H_y^2 \frac{\partial^2 w}{\partial x^2} - H_x^2 \frac{\partial^2 w}{\partial y^2} + H_x^2 \frac{\partial^2 w}{\partial x^2} \right) \quad (13)$$

2.4 Hamilton's principle

The motion equations of DBGS under 2D-magnetic field and biaxial in-plane pre-load can be derived by Hamilton's principles as follows [25]:

$$\int_{t_1}^{t_2} (\delta U + \delta V - \delta K) dt = 0 \quad (14)$$

where δU is the virtual strain energy, δV is the virtual work done by external applied forces and δK is the virtual kinetic energy.

Using Eq. (14) by parts and setting the coefficient of mechanical displacement to zero lead to the following motion equations:

$$\frac{\partial N_{xx}}{\partial x} + \frac{\partial N_{xy}}{\partial y} = m_0 \frac{\partial^2 u}{\partial t^2} \quad (15)$$

$$\frac{\partial N_{xy}}{\partial x} + \frac{\partial N_{yy}}{\partial y} = m_0 \frac{\partial^2 v}{\partial t^2} \quad (16)$$

$$\begin{aligned} & \frac{\partial^2 M_{xx}}{\partial x^2} + 2 \frac{\partial^2 M_{xy}}{\partial x \partial y} + \frac{\partial^2 M_{yy}}{\partial y^2} + q + \frac{\partial}{\partial x} \left(N_{xx} \frac{\partial w}{\partial x} \right) + \frac{\partial}{\partial y} \left(N_{yy} \frac{\partial w}{\partial y} \right) \\ & + \frac{\partial}{\partial x} \left(N_{xy} \frac{\partial w}{\partial y} \right) + \frac{\partial}{\partial y} \left(N_{xy} \frac{\partial w}{\partial x} \right) = m_0 \frac{\partial^2 w}{\partial t^2} - m_2 \left(\frac{\partial^4 w}{\partial t^2 \partial x^2} + \frac{\partial^4 w}{\partial t^2 \partial y^2} \right) \end{aligned} \quad (17)$$

where q is lateral force caused by Pasternak medium and magnetic field and m_0, m_2 are mass moments of inertia that defines as:

$$(m_0, m_2) = \int_{-h/2}^{+h/2} \rho(1, z^2) dz \quad (18)$$

$$q = q_{\text{Pasternak}} + q_{\text{magnetic}} \quad q_{\text{Pasternak}} = -k_w w + k_g \nabla^2 w \quad (19)$$

Substituting Eqs. (1) and (4) into Eq. (17) the governing equation of motion in terms of transverse displacements yields:

$$\begin{aligned} & -D_{11} \frac{\partial^4 w_i}{\partial x^4} - 2(D_{12} + 2D_{33}) \frac{\partial^4 w_i}{\partial y^2 \partial x^2} - D_{22} \frac{\partial^4 w_i}{\partial y^4} - P_i \frac{\partial^2 w_i}{\partial x^2} + (e_0 a)^2 P_i \frac{\partial^4 w_i}{\partial x^4} + (e_0 a)^2 P_i \frac{\partial^4 w_i}{\partial y^2 \partial x^2} - k_i P_i \frac{\partial^2 w_i}{\partial y^2} \\ & + (e_0 a)^2 k_i P_i \frac{\partial^4 w_i}{\partial y^2 \partial x^2} + (e_0 a)^2 k_i P_i \frac{\partial^4 w_i}{\partial y^4} + 4\eta H_x H_y h \frac{\partial^2 w_i}{\partial y \partial x} + \eta H_y^2 h \left(\frac{\partial^2 w_i}{\partial y^2} - \frac{\partial^2 w_i}{\partial x^2} \right) - \eta H_x^2 h \left(\frac{\partial^2 w_i}{\partial y^2} - \frac{\partial^2 w_i}{\partial x^2} \right) \\ & - 4(e_0 a)^2 \eta H_x H_y h \left(\frac{\partial^2 w_i}{\partial y^3 \partial x} + \frac{\partial^2 w_i}{\partial y \partial x^3} \right) - (e_0 a)^2 \eta H_y^2 h \left(\frac{\partial^4 w_i}{\partial y^4} - \frac{\partial^4 w_i}{\partial x^4} \right) + (e_0 a)^2 \eta H_x^2 h \left(\frac{\partial^4 w_i}{\partial y^4} - \frac{\partial^4 w_i}{\partial x^4} \right) \\ & - k_w w + (e_0 a)^2 k_w \left(\frac{\partial^2 w_i}{\partial x^2} + \frac{\partial^2 w_i}{\partial y^2} \right) + k_g \left(\frac{\partial^2 w_i}{\partial x^2} + \frac{\partial^2 w_i}{\partial y^2} \right) - (e_0 a)^2 k_g \left(\frac{\partial^4 w_i}{\partial x^4} + 2 \frac{\partial^4 w_i}{\partial y^2 \partial x^2} + \frac{\partial^4 w_i}{\partial y^4} \right) \\ & + K_i - (e_0 a)^2 \left(\frac{\partial^2 K_i}{\partial x^2} + \frac{\partial^2 K_i}{\partial y^2} \right) + N_x^T \frac{\partial^2 w_i}{\partial x^2} + N_y^T \frac{\partial^2 w_i}{\partial y^2} = m_0 \frac{\partial^2 w_i}{\partial t^2} - (e_0 a)^2 m_0 \left(\frac{\partial^4 w_i}{\partial t^2 \partial x^2} + \frac{\partial^4 w_i}{\partial t^2 \partial y^2} \right) \\ & - m_2 \left(\frac{\partial^4 w_i}{\partial t^2 \partial x^2} + \frac{\partial^4 w_i}{\partial t^2 \partial y^2} \right) + (e_0 a)^2 m_2 \left(\frac{\partial^4 w_i}{\partial x^4} + 2 \frac{\partial^4 w_i}{\partial y^2 \partial x^2} + \frac{\partial^4 w_i}{\partial y^4} \right) \end{aligned} \quad (20)$$

where superscript i ($i = 1, 2$) indicates the number of layers, D_{ii} are various bending rigidities and K_i represents the effect of elastic medium between two layers which are:

$$D_{ii} = \frac{E_{ii}h^3}{12(1-\nu_{12}\nu_{21})} \quad i = x, y$$

$$D_{33} = \frac{G_{12}h^3}{12}$$

$$D_{12} = \frac{E_{22}\nu_{21}h^3}{12(1-\nu_{12}\nu_{21})}$$

$$K_i = \begin{cases} \left. \begin{aligned} & -k_w(w_1 - w_2) + ((e_0a)^2 k_w + k_g) \left(\frac{\partial^2(w_1 - w_2)}{\partial x^2} + \frac{\partial^2(w_1 - w_2)}{\partial y^2} \right) \\ & - (e_0a)^2 k_g \left(\frac{\partial^4(w_1 - w_2)}{\partial x^4} + 2 \frac{\partial^4(w_1 - w_2)}{\partial y^2 \partial x^2} + \frac{\partial^4(w_1 - w_2)}{\partial y^4} \right) \end{aligned} \right\} i = 1 \\ \left. \begin{aligned} & -k_w(w_2 - w_1) + ((e_0a)^2 k_w + k_g) \left(\frac{\partial^2(w_2 - w_1)}{\partial x^2} + \frac{\partial^2(w_2 - w_1)}{\partial y^2} \right) \\ & - (e_0a)^2 k_g \left(\frac{\partial^4(w_2 - w_1)}{\partial x^4} + 2 \frac{\partial^4(w_2 - w_1)}{\partial y^2 \partial x^2} + \frac{\partial^4(w_2 - w_1)}{\partial y^4} \right) \end{aligned} \right\} i = 2 \end{cases} \quad (22)$$

3 SOLUTION PROCEDURE

The DQM is a numerical discretization technique for approximation of derivatives that calculates the variables in discrete points as a weighted linear sum of the function values at all discrete points chosen in the solution domain of the spatial variable [26]. Consider a function Q (representing u , v and w) of the variables in the domain with $N_x \times N_y$ grid points along x and y axes, respectively. Then, the first-order partial derivative of the function $Q(x, y)$ may be approximated by [27]

$$\left(\frac{\partial Q(x, y)}{\partial x} \right)_{x=x_i, y=y_j} = \sum_{k=1}^{N_x} A_{x,ik} Q(x_k, y_j)$$

$$\left(\frac{\partial Q(x, y)}{\partial y} \right)_{x=x_i, y=y_j} = \sum_{k=1}^{N_y} A_{y,jk} Q(x_i, y_k)$$

where A_x, A_y represents the weighting coefficient of the first order partial derivative. The weighting coefficients for higher order derivatives can be obtained by:

$$\left(\frac{\partial^2 Q(x, y)}{\partial x^2} \right) = A_{x,im} A_{x,mk} Q_{kj} = B_{x,ik} Q_{kj}$$

$$\left(\frac{\partial^3 Q(x, y)}{\partial x^3} \right) = A_{x,im} B_{x,mk} Q_{kj} = C_{x,ik} Q_{kj}$$

$$\left(\frac{\partial^4 Q(x, y)}{\partial x^4} \right) = A_{x,im} C_{x,mk} Q_{kj} = D_{x,ik} Q_{kj}$$

where B, C and D are the weighting coefficient of second, third and fourth order of partial derivatives, respectively, and weighting coefficients in y direction are similar. Substituting Eqs. (23) and (24) into the governing equation turns it into a set of algebraic equations expressed as:

$$\begin{aligned}
 & -D_{11} \sum_{k=1}^{N_x} D_{x,ik} w_i(x_k, y_j) - 2(D_{12} + 2D_{33}) \sum_{k=1}^{N_x} \sum_{m=1}^{N_y} B_{x,ik} B_{y,jm} w_i(x_k, y_m) - D_{22} \sum_{m=1}^{N_y} D_{y,jm} w_i(x_m, y_j) - P_i \sum_{k=1}^{N_x} B_{x,ik} w_i(x_k, y_j) \\
 & + (e_0 a)^2 P_i \sum_{k=1}^{N_x} D_{x,ik} w_i(x_k, y_j) + (e_0 a)^2 P_i \sum_{k=1}^{N_x} \sum_{m=1}^{N_y} B_{x,ik} B_{y,jm} w_i(x_k, y_m) - k_i P_i \sum_{m=1}^{N_y} B_{y,jm} w_i(x_m, y_j) \\
 & + (e_0 a)^2 k_i P_i \sum_{k=1}^{N_x} \sum_{m=1}^{N_y} B_{x,ik} B_{y,jm} w_i(x_k, y_m) + (e_0 a)^2 k_i P_i \sum_{m=1}^{N_y} D_{y,jm} w_i(x_m, y_j) + 4\eta H_x H_y h \sum_{k=1}^{N_x} \sum_{m=1}^{N_y} A_{x,ik} A_{y,jm} w_i(x_k, y_m) \\
 & + \eta H_y^2 h \left(\sum_{m=1}^{N_y} B_{y,jm} w_i(x_m, y_j) - \sum_{k=1}^{N_x} B_{x,ik} w_i(x_k, y_j) \right) - \eta H_x^2 h \left(\sum_{m=1}^{N_y} D_{y,jm} w_i(x_m, y_j) - \sum_{k=1}^{N_x} B_{x,ik} w_i(x_k, y_j) \right) \\
 & - 4(e_0 a)^2 \eta H_x H_y h \left(\sum_{k=1}^{N_x} \sum_{m=1}^{N_y} A_{x,ik} C_{y,jm} w_i(x_k, y_m) + \sum_{k=1}^{N_x} \sum_{m=1}^{N_y} C_{x,ik} A_{y,jm} w_i(x_k, y_m) \right) \\
 & - (e_0 a)^2 \eta H_y^2 h \left(\sum_{m=1}^{N_y} D_{y,jm} w_i(x_m, y_j) - \sum_{k=1}^{N_x} D_{x,ik} w_i(x_k, y_j) \right) + (e_0 a)^2 \eta H_x^2 h \left(\sum_{m=1}^{N_y} D_{y,jm} w_i(x_m, y_j) - \sum_{k=1}^{N_x} D_{x,ik} w_i(x_k, y_j) \right) \\
 & - k_w w_i(x_i, y_j) + (e_0 a)^2 k_w \left(\sum_{k=1}^{N_x} B_{x,ik} w_i(x_k, y_j) + \sum_{m=1}^{N_y} B_{y,jm} w_i(x_m, y_j) \right) + k_g \left(\sum_{k=1}^{N_x} B_{x,ik} w_i(x_k, y_j) + \sum_{m=1}^{N_y} B_{y,jm} w_i(x_m, y_j) \right) \\
 & - (e_0 a)^2 k_g \left(\sum_{k=1}^{N_x} D_{x,ik} w_i(x_k, y_j) + 2 \sum_{k=1}^{N_x} \sum_{m=1}^{N_y} B_{x,ik} B_{y,jm} w_i(x_k, y_m) + \sum_{m=1}^{N_y} D_{y,jm} w_i(x_m, y_j) \right) + K_i \\
 & - (e_0 a)^2 \left(\sum_{k=1}^{N_x} B_{x,ik} K_i(x_k, y_j) + \sum_{m=1}^{N_y} B_{y,jm} K_i(x_m, y_j) \right) + N_x^T \sum_{k=1}^{N_x} B_{x,ik} w_i(x_k, y_j) + N_y^T \sum_{m=1}^{N_y} B_{y,jm} w_i(x_m, y_j) \\
 & = m_0 \ddot{w}_i(x_i, y_j) - (e_0 a)^2 m_0 \left(\sum_{k=1}^{N_x} B_{x,ik} \ddot{w}_i(x_k, y_j) + \sum_{m=1}^{N_y} B_{y,jm} \ddot{w}_i(x_m, y_j) \right) - m_2 \left(\sum_{k=1}^{N_x} B_{x,ik} \ddot{w}_i(x_k, y_j) + \sum_{m=1}^{N_y} B_{y,jm} \ddot{w}_i(x_m, y_j) \right) \\
 & + (e_0 a)^2 m_2 \left(\sum_{k=1}^{N_x} D_{x,ik} \ddot{w}_i(x_k, y_j) + 2 \sum_{k=1}^{N_x} \sum_{m=1}^{N_y} B_{x,ik} B_{y,jm} \ddot{w}_i(x_k, y_m) + \sum_{m=1}^{N_y} D_{y,jm} \ddot{w}_i(x_m, y_j) \right)
 \end{aligned} \tag{25}$$

In order to solve the time derivatives of Eq. (25), the dynamic displacement vector w is expanded as:

$$w(x, y, t) = w(x, y) e^{\omega t} \tag{26}$$

where ω represents the frequency of DBGs under magnetic field. In order to carry out the matrix multiplication, mathematical product (Kronecker) is applied. Using Kronecker product of matrices [28-29] which is defined as:

$$A \otimes C = (a_{ij} C)_{ij} \tag{27}$$

Therefore, coupled formulations can be expressed as:

$$\begin{aligned}
 & -D_{11}(I_y \otimes D_x)w_i - 2(D_{12} + 2D_{33})(B_y \otimes B_x)w_i - D_{22}(D_y \otimes I_x)w_i - P_i(I_y \otimes B_x)w_i + (e_0a)^2 P_i(I_y \otimes D_x)w_i \\
 & + (e_0a)^2 P_i(B_y \otimes B_x)w_i - k_i P_i(B_y \otimes I_x)w_i + (e_0a)^2 k_i P_i(B_y \otimes B_x)w_i + (e_0a)^2 k_i P_i(D_y \otimes I_x)w_i \\
 & + 4\eta H_x H_y h(A_y \otimes A_x)w_i + \eta H_y^2 h((B_y \otimes I_x)w_i - (I_y \otimes B_x)w_i) - \eta H_x^2 h((D_y \otimes I_x)w_i - (I_y \otimes B_x)w_i) \\
 & - 4(e_0a)^2 \eta H_x H_y h((C_x \otimes A_x)w_i + (A_y \otimes C_x)w_i) - (e_0a)^2 \eta H_y^2 h((D_y \otimes I_x)w_i - (I_y \otimes D_x)w_i) \\
 & + (e_0a)^2 \eta H_x^2 h((D_y \otimes I_x)w_i - (I_y \otimes D_x)w_i) - k_w(I_y \otimes I_x)w_i + (e_0a)^2 k_w((I_y \otimes B_x)w_i + (B_y \otimes I_x)w_i) \\
 & + k_g((I_y \otimes B_x)w_i + (B_y \otimes I_x)w_i) - (e_0a)^2 k_g((I_y \otimes D_x)w_i + 2(B_y \otimes B_x)w_i + (D_y \otimes I_x)w_i) + K_i \\
 & - (e_0a)^2 ((I_y \otimes B_x)K_i + (B_y \otimes I_x)K_i) + N_x^T(I_y \otimes B_x)w_i + N_y^T(B_y \otimes I_x)w_i = m_0(I_y \otimes I_x)w_i \omega^2 \\
 & - (e_0a)^2 m_0((I_y \otimes B_x)w_i + (B_y \otimes I_x)w_i) \omega^2 - m_2((I_y \otimes B_x)w_i + (B_y \otimes I_x)w_i) \omega^2 \\
 & + (e_0a)^2 m_2((I_y \otimes D_x)w_i + 2(B_y \otimes B_x)w_i + (D_y \otimes I_x)w_i) \omega^2
 \end{aligned} \tag{28}$$

Introducing the following dimensionless quantities figures expressed in general form:

$$\begin{aligned}
 \bar{w} &= \frac{w}{h} & \xi_x &= \frac{x}{L_x} & \xi_y &= \frac{y}{L_y} & \beta &= \frac{L_y}{L_x} \\
 \eta_y &= \frac{h}{L_y} & \eta_x &= \frac{h}{L_x} & \bar{D}_{ii} &= \frac{D_{ii}}{E_{11}L_y^3} \quad i = 1, \dots, 3 & \bar{D}_{12} &= \frac{D_{12}}{E_{11}L_y^3} \\
 \bar{k}_w &= \frac{k_w L_y}{E_{11}} & \bar{k}_g &= \frac{k_g}{L_y E_{11}} & \bar{N}_j^T &= \frac{N_j^T}{L_y E_{11}} \quad j = x, y & \bar{P}_j &= \frac{P_j}{L_y E_{11}} \quad j = x, y \\
 \mathfrak{R} &= \frac{\eta H^2}{E_{11}} & \mu &= \left(\frac{e_0 a}{L_x}\right)^2 & \bar{t} &= \frac{t}{L_y} \sqrt{\frac{E_{11}}{\rho}}
 \end{aligned} \tag{29}$$

Substituting Eqs. (29) into Eq. (26), can be expressed in matrix form which is called eigen value problem as:

$$\left[[K] + \omega^2 [M] \right] \{V\} = 0 \tag{30}$$

4 RESULTS AND DISCUSSIONS

In this study, the effect of 2D-magnetic field and biaxial in-plane pre-load on thermo-nonlocal vibration of a orthotropic DBGS resting on Pasternak foundation is investigated. The orthotropic mechanical properties of GS are listed in Table 1 [30].

Table 1
Mechanical Thermal and Geometrical properties of orthotropic GS for Armchair structure [30].

Type of Structure	Mechanical properties				Thermal properties			Geometrical properties			
	E_{11} (TPa)	E_{22} (TPa)	G_{12} (TPa)	ν_{12} ν_{21}	ρ (kg / m ³)	T (°K)	α_{11} (1 / °K)	α_{22} (1 / °K)	L_x (nm)	L_y (nm)	h (nm)
Armchair Sheet	2.434	2.473	1.039	0.197	6316	300	2.2E-6	2.0E-6	9.519	4.844	0.129

The effects of magnetic field direction, magnitude of magnetic field, different case of in-plane pre-loads on couple system and aspect ratio investigated in this study. Fig. 2 expresses dimensionless Frequency versus magnetic angle for different dimensionless nonlocal parameter. Since $\beta=1$ in this figure ($\beta=L_y/L_x=1$), the geometric symmetric is at $\theta = 45^\circ$ and it is the reason of the symmetric dimensionless frequency at this angle. Also, it can be

seen from this figure that with increasing magnetic angle to 45° dimensionless frequency decreases and due to symmetry from 45° to 90° , dimensionless frequency increases. This figure shows the effect of nonlocal parameter on dimensionless frequency versus angle of magnetic field where increasing nonlocal parameter caused to decrease dimensionless frequency. When the magnetic field applied in x or y directions, the difference between dimensionless frequency is low and at $\theta = 45^\circ$ this difference is maximum. Varying dimensionless frequency versus change of dimensionless magnetic parameter (\hat{A}) for different angles is shown in Figs. 3 and 4, where the magnetic parameter is considered as linear and logarithmic in Figs. 3 and 4, respectively. It is observed that with increasing magnetic parameter, dimensionless frequency increases and the effect of magnetic angle is remarkable at higher magnetic values.

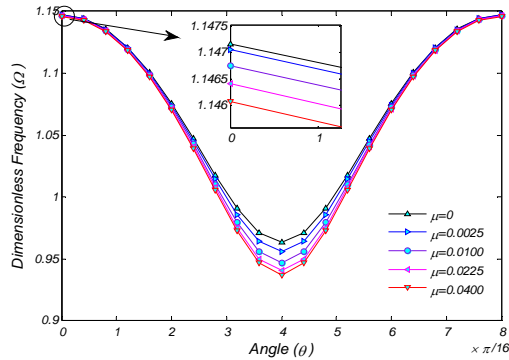


Fig. 2
Effect of magnetic field direction with change of nonlocal parameter.

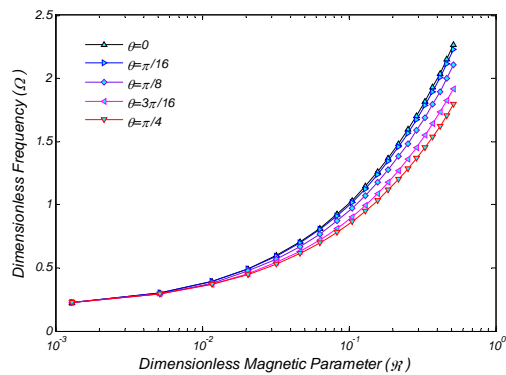


Fig. 3
Dimensionless frequency versus logarithmic dimensionless magnetic field for different angle of magnetic field.

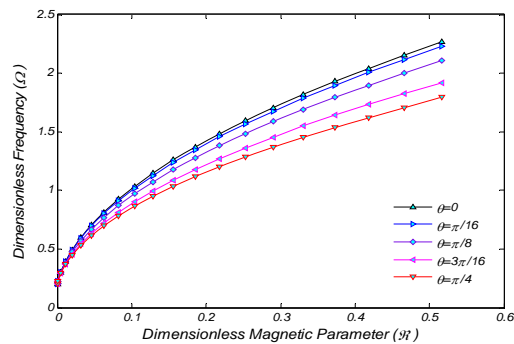


Fig. 4
Dimensionless frequency versus linear dimensionless magnetic field for different angle of magnetic field.

In this study, four typical loadings are considered for DBGS as (see Fig. 5):

1. In-phase x - Pre-loads and In-Phase y - Pre-loads (IX-IY): when the in-plane pre-load on x -direction for both layers are synchrony and in-plane pre-load on y -direction for both layers are synchrony (case 1).
2. In-phase x - Pre-loads and Out-of-Phase y - Pre-loads (IX-OY): when the in-plane pre-load on x -direction for both layers are synchrony and in-plane pre-load on y -direction for both layers are asynchrony (case 2).

3. Out-of-phase x - Pre-loads and In-Phase y - Pre-loads (OX-IY): when the in-plane pre-load on x -direction for both layers are asynchrony and in-plane pre-load on y -direction for both layers are synchrony (case 3).
 4. Out-of-phase x - Pre-load and Out-of-Phase y - Pre-load (OX-OY): when the in-plane pre-load on x -direction for both layers are asynchrony and in-plane pre-load on y -direction for both layers are asynchrony (case 4).
- where at these cases $N_{yy1} = k_1 \times N_{xx1}$ and $N_{yy2} = k_2 \times N_{xx2}$.

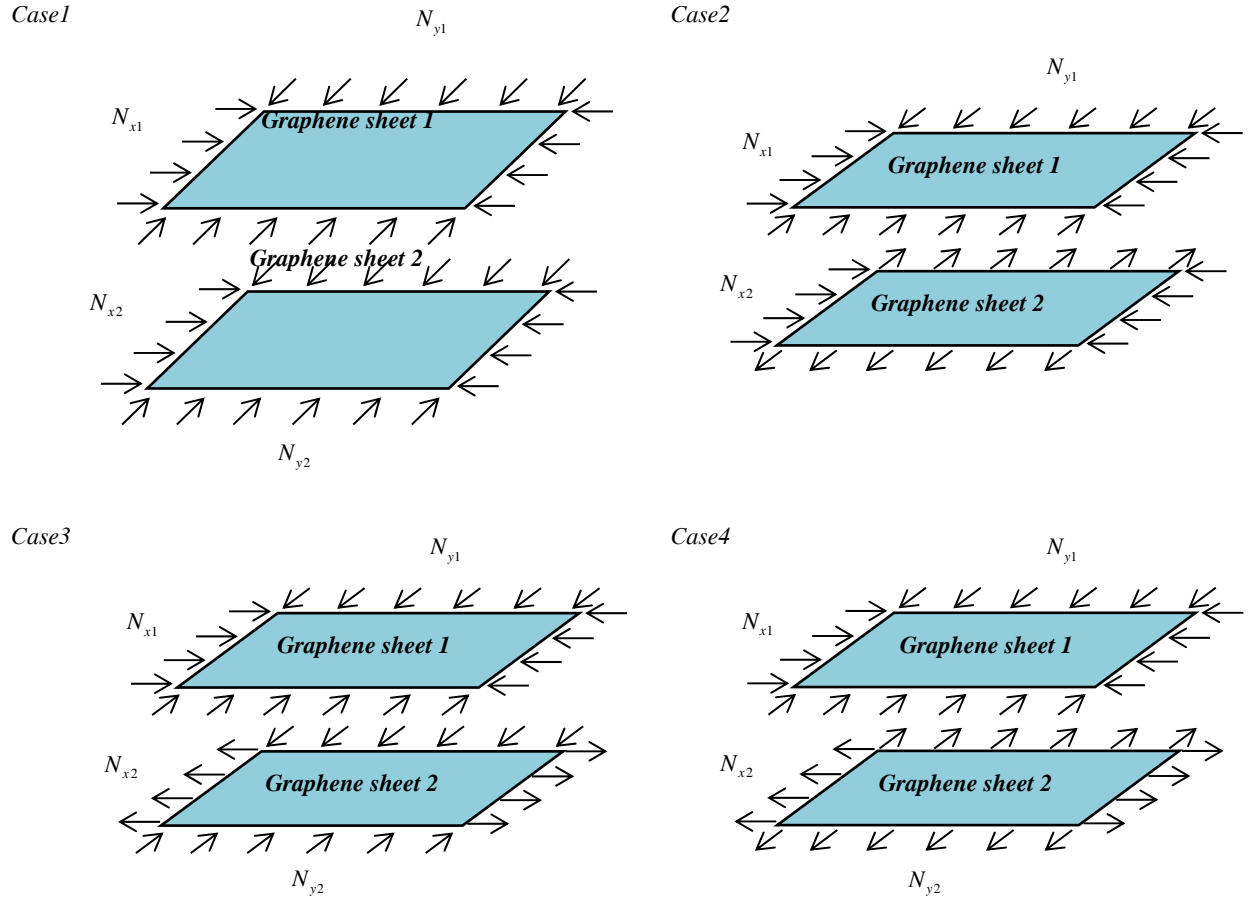


Fig. 5
Four typical loadings on each of graphene layer.

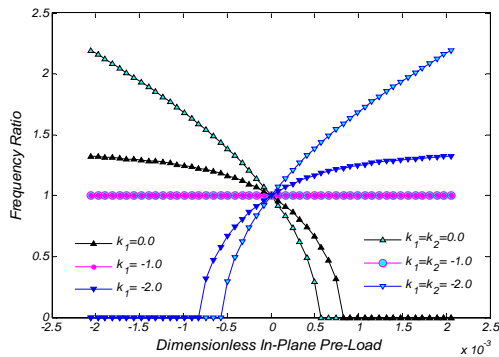


Fig.6
Frequency ratio versus dimensionless in-plane pre-loads for case (IX-IY).

Fig. 6 indicates frequency ratio versus dimensionless in-plane pre-load for case 1 (IX-IY) where in-plane pre-loads act on one layer ($N_{xx2} = N_{yy2} = 0$) and two layers. In common state $k = -1$, frequency ratio with varying in-

plane pre-load is constant and equal to 1. It is found that three states are intersect in $\bar{P} = 0$, also it can be seen that in $k = -1$, frequency is constant or frequency with pre-loads is equal to frequency without pre-loads because of:

$$\text{Frequency Ratio} = \frac{\text{Frequency with in-plane pre-load}}{\text{Frequency without in-plane pre-load}}$$

Fig. 7 demonstrates frequency ratio versus dimensionless in-plane pre-load for case 2 (IX-OY). It is found that similar to case (IX-IY) whole states are converge to (0, 1) point. In this case, positive and negative magnitudes of load factors (k_1, k_2) are same and with increasing its value instability region increases. Effect of load condition on frequency ratio for case 3 (OX-IY) is indicated in Fig. 8 where same as previous figures, curves are converge in (0, 1) point. Fig. 9 expresses the effect of load condition on frequency ratio for case 4 (OX-OY). It is found that the stability and frequency ratio increase with decrease of load factor from positive to negative values. Whole curves converge in $\bar{P} = 0$ and symmetric occurs in this position. At state $k_1 = k_2 = -1$ the frequency ratio is maximum and equal 1. Finally, when in-plane pre-load on x - and y -direction for both layers are asynchrony or synchrony, it can be concluded that in $k = -1$ the effect of in-plane pre-loading can be ignored, otherwise it can not be ignored.

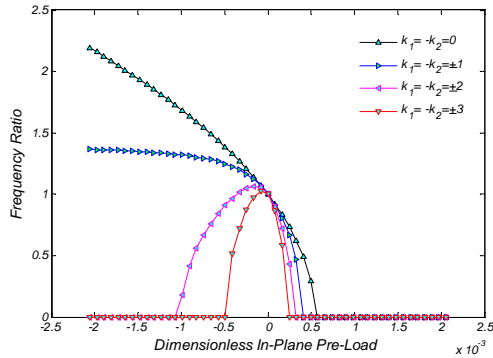


Fig. 7
Effect of load condition on frequency ratio for case (IX-OY).

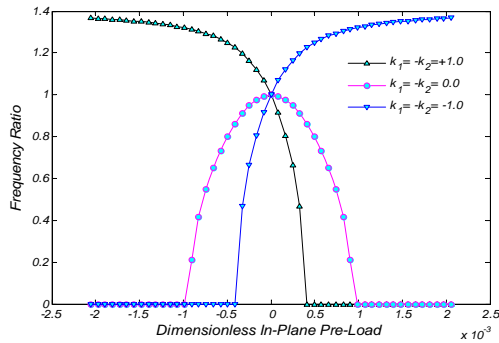


Fig. 8
Effect of load condition on frequency ratio for case (OX-IY).

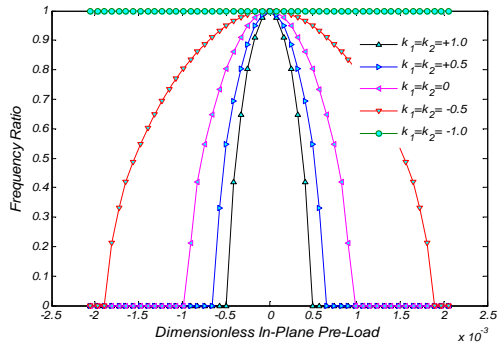


Fig. 9
Effect of load condition on frequency ratio for case (OX-OY).

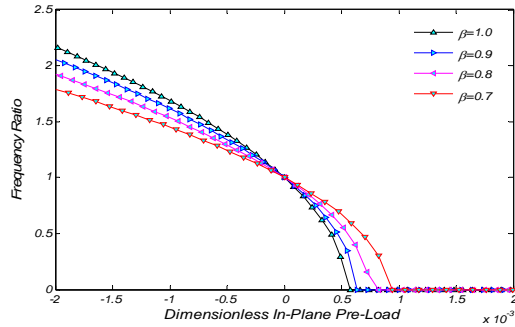


Fig. 10
Effect of aspect ratio on frequency ratio with change of in-plane pre-loads.

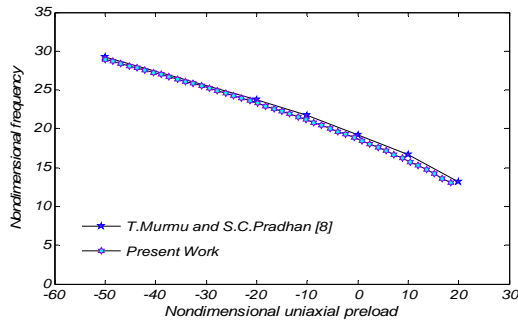


Fig. 11
Comparison between present results with those presented by Murmu and pradhan [8].

Fig. 10 shows the frequency ratio versus dimensionless in-plane pre-load for different aspect ratio (β). With decreasing aspect ratio, the length of nanoplate in y -direction decreases and nanoplate convert to nanobeam. With decreasing the aspect ratio, frequency ratio decreases for tensile in-plane pre-load and frequency ratio increases for compressive in-plane pre-load. In order to validate present study, a simplified case of the analysis is considered a single layer GS under uniaxial pre-stressed conditions by T. Murmu and S. C. Pradhan [8], in which nondimensional frequency versus nondimensional uniaxial pre-load is plotted for local vibration. The results presented by [8] are compared with the results of this investigation in Fig. 11. This figure demonstrates there is good agreement between them.

5 CONCLUSION

Transverse vibration analysis of DBGS based on the nonlocal continuum theory subjected to 2D-magnetic field and combined biaxial in-plane pre-loadings was developed. The Pasternak interaction forces between adjacent layers were also taken into account in this study. The effects of load conditioning, magnetic field angle, nonlocal parameter and aspect ratio on couple system frequency were investigated. In general, results showed that vibration behavior in any load condition is unique and depends on in-phase or out-of-phase loading on x - and y -direction on two layers. It was found from figures when in-plane pre-load on x - and y -direction for both layers are synchrony (IX-IY) and asynchrony (OX-OY) in $k = -1$, can ignored in-plane pre-loading effects, and also curves of total figures are converge in (0,1) point. By increasing the magnetic angle to $\theta = 45^\circ$, the dimensionless frequency decreases. The results of this study could be used in optimum design of NEMS/MEMS under magnetic field as a frequency controller.

ACKNOWLEDGMENTS

The authors are grateful to University of Kashan for supporting this work by Grant No. 65475/58.

REFERENCES

- [1] Pradhan S.C., Kumar A., 2010, Vibration analysis of orthotropic graphene sheets embedded in Pasternak elastic medium using nonlocal elasticity theory and differential quadrature method, *Computational Materials Science* **50**: 239-245.
- [2] Murmu T., Adhikari S., 2011, Axial instability of double-nanobeam-systems, *Physics Letters A* **375**: 601-608.
- [3] Murmu T., Adhikari S., 2011, Nonlocal vibration of bonded double-nanoplate-systems, *Composites: Part B* **42**: 1901-1911.
- [4] Singh J.P., Dey S.S., 1990, Transverse vibration of rectangular plates subjected to inplane forces by a difference based vibrational approach, *International Journal of Mechanical Sciences* **32**: 591-599.
- [5] Zhang Y., Liu G., Han X., 2005, Transverse vibrations of double-walled carbon nanotubes under compressive axial load, *Physics Letters A* **340**: 258-266.
- [6] Mustapha K.B., Zhong Z.W., 2010, Free transverse vibration of an axially loaded non-prismatic single-walled carbon nanotube embedded in a two-parameter elastic medium, *Computational Materials Science* **50**: 742-751.
- [7] Karami Khorramabadi M., 2009, Free vibration of functionally graded beams with piezoelectric layers subjected to axial load, *Journal of Solid Mechanics* **1**: 22-28.
- [8] Murmu T., Pradhan S.C., 2009, Vibration analysis of nanoplates under uniaxial prestressed conditions via nonlocal elasticity, *Journal of Applied Physics* **106**: 104301.
- [9] Kiani K., 2012, Vibration analysis of elastically restrained double-walled carbon nanotubes on elastic foundation subjected to axial load using nonlocal shear deformable beam theories, *International Journal of Mechanical Sciences* **68**: 16-34.
- [10] Ajiki H., Ando T., 1993, Electronic states of carbon nanotubes, *Journal of Physical Society of Japan* **62**: 1255-1266.
- [11] Ajiki H., Ando T., 1994, Aharonov-Bohm effect in carbon nanotubes, *Physica B* **201**: 252-349.
- [12] Ajiki H., Ando T., 1996, Energy bands of carbon nanotubes in magnetic fields, *Journal of Physical Society of Japan* **65**: 505-514.
- [13] Saito R., Dresselhaus G., Dresselhaus M.S., 1998, *Physical Properties of Carbon Nanotubes*, Imperial College Press, London.
- [14] O'Connell M.J., 2006, *Carbon Nanotubes: Properties and Applications*, CRC Press, Boca Raton.
- [15] Ghorbanpour Arani A., Amir S., 2011, Magneto-thermo-elastic stresses and perturbation of magnetic field vector in a thin functionally graded rotating disk, *Journal of Solid Mechanics* **3**: 392-407.
- [16] Lu H., Gou J., Leng J., Du S., 2011, Magnetically aligned carbon nanotube in nanopaper enabled shape-memory nanocomposite for high speed electrical actuation, *Applied Physics Letters* **98**: 174105.
- [17] Camponeschi E., Vance R., Al-Haik M., Garmestani H., Tannenbaum R., 2007, Properties of carbon nanotube-polymer composites aligned in a magnetic field, *Carbon* **45**: 2037-2046.
- [18] Bubke K., Gnewuch H., Hempstead M., Hammer J., Green M.L.H., 1997, Optical anisotropy of dispersed carbon nanotubes induced by an electric field, *Applied Physics Letters* **71**: 1906-1908.
- [19] Liu T X., Spencer J.L., Kaiser A.B., Arnold W.M., 2004, Electric-field oriented carbon nanotubes in different dielectric solvents, *Current Applied Physics* **4**: 125-128.
- [20] Kiani K., 2012, Transverse wave propagation in elastically confined single-walled carbon nanotubes subjected to longitudinal magnetic fields using nonlocal elasticity models, *Physica E* **45**: 86-96.
- [21] Murmu T., McCarthy M.A., Adhikari S., 2013, In-plane magnetic field affected transverse vibration of embedded single-layer graphene sheets using equivalent nonlocal elasticity approach, *Composite Structures* **96**: 57-63.
- [22] Timoshenko S., Woinowsky-Krieger S., 1959, *Theory of Plates and Shells*, Second edition, MCGRAW-HILL, London.
- [23] Eringen A.C. 1983, On differential equations of nonlocal elasticity and solutions of screw dislocation and surface waves, *Journal of Applied Physics* **54**: 4703-4710.
- [24] John, K.D., 1984, *Electromagnetics*, McGraw-Hill, Moscow.
- [25] Reddy J.N., 1997, *Mechanics of Laminated Composite Plates, Theory and Analysis*, Chemical Rubber Company, Boca Raton, FL.
- [26] Sherbourne A.N., Pandey M.D., 1991, Differential quadrature method in the buckling analysis of beams and composite plates, *Computers and Structures* **40**: 903-913.
- [27] Bert C.W., Malik M., 1996, Differential quadrature method in computational mechanics: a review, *Applied Mechanics Reviews* **49**: 1-28.
- [28] Chen W., Shu C., He W., Zhong T., 2000, The applications of special matrix products to differential quadrature solution of geometrically nonlinear bending of orthotropic rectangular plates, *Computers and Structures* **74**: 65-76.
- [29] Lancaster P., Timenetsky M., 1985, *The Theory of Matrices with Applications*, second edition, Academic Press Orlando.
- [30] Ghorbanpour Arani A., Kolahchi R., Mosallaie Barzoki A.A., Mozdianfard M.R., Node S.M., 2013, Elastic foundation effect on nonlinear thermo-vibration of embedded double layered orthotropic graphene sheets using differential quadrature method, *Journal of Mechanical Engineering Science: Part C* **227**: 862-879.